

Formatted: Header

Inland lake temperature initialization via **coupled** cycling with atmospheric data assimilation

Stanley G. Benjamin¹, Tatiana G. Smirnova^{2,1}, Eric P. James^{2,1}, Eric J. Anderson³, Ayumi Fujisaki-Manome^{4,5}, John G.W. Kelley⁶, Greg E. Mann⁷, Andrew D. Gronewold⁵, Philip Chu⁸, Sean G.T. Kelley⁹

¹NOAA Global Systems Laboratory, Boulder, CO 80305 USA

²Cooperative Institute for Research in Environmental Science (CIRES), University of Colorado, Boulder, CO 80303 USA

³Civil and Engineering Department, Colorado School of Mines, Golden, CO USA

⁴Cooperative Institute for Great Lakes Research (CIGLR), University of Michigan, Ann Arbor, MI USA

⁵University of Michigan, Ann Arbor, MI USA

⁶NOAA National Ocean Service, Coast Survey Development Laboratory, Durham, NH 03824 USA

⁷NOAA National Weather Service, White Lake, MI, USA

⁸NOAA Great Lakes Environmental Research Laboratory, Ann Arbor, MI, USA

⁹University of Massachusetts, Department of Mathematics and Statistics, Amherst, MA, USA

Correspondence to: Stan Benjamin (stan.benjamin@noaa.gov)

8 Dec 2021 - submitted to Geoscientific Model Development (GMD)

https://gmd.copernicus.org/articles/special_issue1114.html

Special issue I Modelling inland waters in a changing climate (GMD/ESD/TC inter-journal SI).

- Resubmitted with editorial changes – 21 Jan 2022, **21 June 2022**

Formatted: Indent: Left: 0", Hanging: 0.5"

Deleted: .

Abstract. Application of lake models coupled within earth-system prediction models, especially for short-term predictions from days to weeks, requires accurate initialization of lake temperatures. Here, we describe a lake initialization method by **coupled** cycling within an hourly updated weather prediction model to constrain lake temperature evolution. We compare these simulated lake temperature values with other estimates from satellite and in situ and interpolated-SST data sets for a multi-month period in 2021. The lake cycling initialization, now applied to two operational US NOAA weather models, was found to decrease errors in lake temperature from as much as 5-10K (using interpolated-SST data) to about 1-2 K (comparing with available in situ and satellite observations).

Short summary

Application of 1-d lake models coupled within earth-system prediction models will improve accuracy but requires accurate initialization of lake temperatures. Here, we

describe a lake initialization method by coupled cycling within a weather prediction model to constrain lake temperature evolution. We compare these lake temperature values with other estimates and found much reduced errors (down to 1-2 K). The lake cycling initialization is now applied to two operational US NOAA weather models.

1 Introduction

Inclusion of lake representation into numerical weather prediction (NWP) models has become increasingly necessary to further improve representation of atmosphere-surface fluxes of heat and moisture as model grid resolution becomes finer. Representation of lake physics to provide time-varying lake surface properties (e.g., Subin et al, 2012) is essential to improve fluxes of heat, moisture and momentum between the surface and atmosphere (Hostetler et al, 1993, Thiery et al, 2014). Lake representation is part of the overall surface treatment including land-surface models (LSMs) necessary to accurately model the evolution of the planetary boundary layer. Lakes are estimated to cover 3.7% of the global non-glaciated land area (Verpoorter et al, 2014), and they significantly moderate sensible heat and moisture fluxes from this 'land' (i.e., non-ocean) area. Water impoundments (reservoirs) that used to account for about 6% of these 'lake' areas (Downing et al, 2006) have recently increased to 9% (Vanderkelen et al, 2021). Initial conditions for both land and lake surface are an important consideration due to far larger thermal inertia for soil or water than for air. Consequently, incorrect soil or lake initial conditions can result in erroneous heat and moisture fluxes that may persist for days and even weeks (e.g., Dirmeyer et al, 2018). This potential source of error in fluxes is more pronounced for lake areas with far larger thermal inertia and heat storage than even saturated soils.

In operational US NOAA weather prediction models (global and regional) up to this point, daily sea-surface temperature (SST) analyses have been used to specify the surface water temperatures for even small inland lakes. Inland lake temperatures in North America have been obtained by the interpolation of SST values from the ocean and the Laurentian Great Lakes. An alternative is to incorporate one-dimensional (1-d) lake models within NWP models and use coupled cycling forced by atmospheric conditions updated by new observations and continuously simulated 1-d lake models to obtain realistic lake water temperatures (e.g., "cycling"). This cycling to initialize small lakes in NOAA operational regional weather prediction models complements loose coupling with a 3-d hydrodynamical lake model for the Laurentian Great Lakes as described elsewhere in Fujisaki-Manome et al 2020.

Lake representation (via one-dimensional (1-d) models, as in LSMs) within NWP models is beneficial by providing a first-order accurate lagged effect of the seasonal variation in temperature, with lake water remaining colder than nearby land in spring and warmer in autumn. The outcomes are desirable, as described by Balsamo et al (2012), for instance by accurately representing increased evaporative fluxes in the fall.

Deleted: the US,

Deleted: NWP

Deleted: have used coarse-resolution

Deleted: the ocean and the Laurentian Great Lakes for the entire forecast period. However, given the resolution, the ...

Deleted: for bays, sounds, and smaller non-Great Lakes ...

97 Thus, use of a 1-d lake model ~~has the potential to improve~~ over land representation by
98 capturing this slower seasonal response.

99
100 However, lake temperature initialization ~~from SST~~ (e.g., Mallard et al, 2015) can
101 exaggerate this seasonal slower response. Shallow lakes warm more slowly in spring
102 than surrounding land, but more quickly than nearby deeper lakes. Even in summer, it
103 will take at least 1-2 weeks for ~~cycled~~ 1-d models to adjust from values interpolated from
104 deeper-lake temperatures to become more realistic for shallow lakes. Therefore, lake
105 temperature initialization becomes the most important factor to accurately simulate
106 sensible and latent heat fluxes from lakes for short to medium-range NWP, more so
107 than the use of the lake model itself. One option to solve the lake initialization problem
108 is to use a model-based climatology for seasonal variation of lake temperatures
109 (Balsamo et al (2012) and Balsamo (2013), ~~ECMWF using a 1-d lake model forced by~~
110 ~~reanalysis data. The 1-d lake model used by ECMWF for this method is the 2-layer~~
111 ~~FLake (Freshwater Lake Model) model (Mironov et al, 2010, Balsamo et al, 2012,~~
112 ~~Boussetta et al, 2021) and also implemented into their Integrated Forecast System (IFS)~~
113 ~~in 2015. A similar technique was applied by Mironov et al (2010) using FLake for the~~
114 ~~COSMO model. Kourzeneva et al (2012a) describe application of 20-year reanalysis~~
115 ~~data to create a global lake climatology dataset using FLake.~~ This technique avoids a
116 new spin-up with each new run, but cannot capture unique weather regime variations in
117 a given region and time. ~~The UK Met Office uses satellite data to update their lake~~
118 ~~surface water temperatures using the previous day values as a background (Fiedler et~~
119 ~~al, 2014). Another option to solve the lake initialization problem, described here, is lake~~
120 ~~temperature evolution, referred to as "lake cycling", with the ongoing 1-d lake prediction~~
121 ~~within an NWP model,~~ a cost-free option if the atmospheric conditions are relatively
122 accurate.

123
124 Data assimilation for land-surface fields (e.g., soil temperature, soil moisture, snow
125 cover, snow water equivalent, snow temperature) has been very beneficial for improved
126 short-range weather prediction accuracy (e.g., Balsamo and Mahfouf, 2020, Muñoz-
127 Sabater et al, 2019, Benjamin et al, 2022, others), but lake temperature has not been a
128 part of this surface data assimilation. In December 2020, the NOAA 13-km Rapid
129 Refresh (RAP) and 3-km High-Resolution Rapid Refresh (HRRR) implemented an
130 interactive small-lake multi-layer 1-d lake model, the first NOAA weather models to do
131 so. The lake coverages for the HRRR ~~model is~~ shown in Fig. 1, ~~(RAP model lake~~
132 ~~coverage not shown).~~ The HRRR and RAP weather models are coupled with the 10-
133 layer Community Land Model (CLM) version 4.5 lake model, (Subin et al, 2012, Mallard
134 et al, 2015), an option within the community Weather Research and Forecast model
135 (WRF, Skamarock et al, 2019). The CLM lake model is a 1-d thermal diffusion model
136 allowing 2-way coupling with the atmosphere. ~~Virtually no additional computational cost~~
137 ~~(<0.1 %) was added by use of the CLM lake model within the HRRR model.~~ To
138 initialize small-lake temperatures in the RAP and HRRR, all lake variables have been
139 evolving (e.g., "lake cycling") since summer 2018 depending on the cycled atmospheric
140 conditions and the lake model physics as discussed in section 4. ~~This cycling is similar~~

Formatted: Header

Deleted: improves

Deleted: is still a problem. Use of spatial interpolation to smaller lakes from larger (and deeper) lakes, or from the ocean, for lake initialization

Deleted:)) using a 1-d lake model forced by reanalysis data....

Deleted: Another option, described here, is lake cycling...

Deleted: and RAP models are

Deleted: .

Deleted: ECMWF had taken a similar approach earlier to improve their overall surface modeling treatment

Deleted: implementing

Deleted: 2-layer FLake (Freshwater Lake Model)

Deleted: (Mironov et al, 2010, Balsamo et al, 2012, Boussetta et al, 2021) into their Integrated Forecast System (IFS) in 2015.

to the land-surface cycling in HRRR and RAP as described by Benjamin et al (2022). The 1-d lake model cannot represent 3-d hydrodynamical processes in larger bodies of water. Thus, a second major improvement in 2020 with lake representation in the NOAA 3-km HRRR model occurred with the implementation of lagged data coupling with the 3-d hydrodynamic-ice model for the much larger Laurentian Great Lakes as described by Fujisaki-Manome et al (2020).

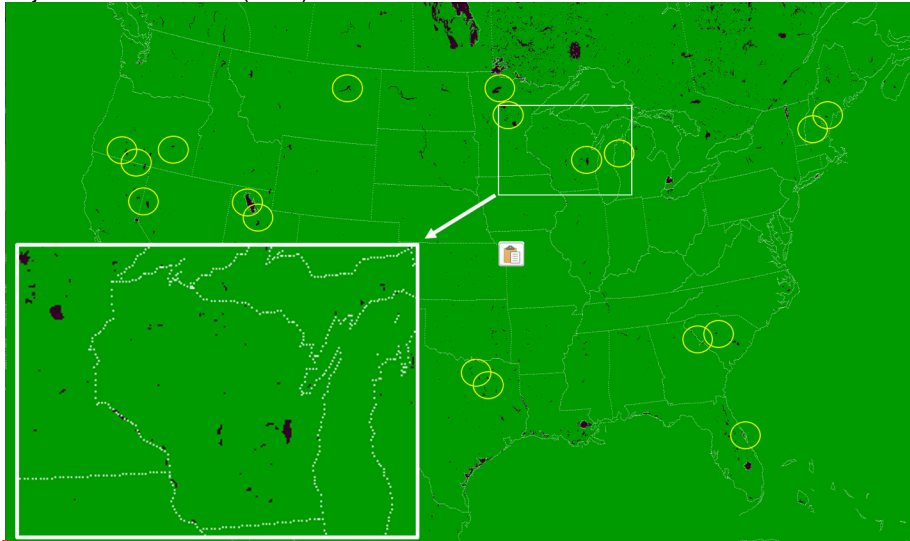
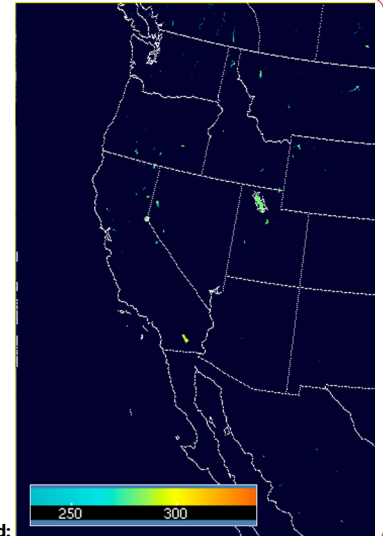


Fig. 1. Small-lake areas for the 3-km HRRR domain using the MODIS 0.15" resolution data for land/water and lake information. Only small-lake areas treated in HRRR by the 1-d CLM lake model are shown. A zoomed-in insert for HRRR small-lake coverage in the vicinity of the state of Wisconsin is shown in the lower left. Out of the 1,900,000 grid points in this HRRR CONUS domain, 12,305 of them (~0.6%) are for small lakes (excluding the 5 Laurentian Great Lakes treated by separate coupling as described in text). Lakes circled in yellow were related to problem reports from US National Weather Service Forecast Offices on nearby deficient 2 m air temperature or dewpoint forecasts in NOAA hourly updated models as discussed in section 2.

Here, we describe the design and results of a unique approach to inland small-lake initialization by cycling with hourly updating of atmospheric conditions (clouds/radiation, near-surface temperature/moisture/winds). This lake initialization via cycling is an important component of earth-system coupled modeling for effective NWP, with goals to improve prediction of 2-m (air) temperature and moisture, cloud, boundary-layer conditions, and precipitation for situational awareness enabling short-range decision making (e.g., aviation, severe weather, hydrology, energy).

2 The Lake Initialization Problem

Formatted: Header



Deleted:

Deleted: 1a.... Small-lake (green to yellow)...areas for the 3-km HRRR domain using the MODIS 0.15" resolution data for land/water and lake information. Color corresponds to top-level lake temperature (K) at temperature (K) at 01z 15 Oct 2019. ... [1]

Formatted: Font: Not Italic



Deleted:

Deleted:

210
211 For the NOAA hourly updated mesoscale models, used frequently for short-range
212 weather prediction, poor 2-m air temperature and/or dewpoint forecasts have been
213 reported intermittently during 2004-2019 by the US National Weather Service (NWS) in
214 the vicinity of inland lakes (Fig. 1). These hourly updated models included the Rapid
215 Update Cycle (RUC, Benjamin et al, 2004) with horizontal grid spacing decreasing from
216 40-km to 20-km to 13-km (Benjamin et al, 2010), succeeded by the 13-km Rapid
217 Refresh (RAP) and 3-km High-Resolution Rapid Refresh (HRRR, Benjamin et al, 2016,
218 Dowell et al, 2022 (D22), James et al, 2022 (J22)). Many of these reported systematic
219 deficiencies from the US NWS were for the 2.5-km NOAA Real-Time Mesoscale
220 Analysis (RTMA, Pondeva et al. 2011), using 1-h forecasts from the 3-km HRRR as a
221 background. The most common report was too-low 2-m air temperatures near inland
222 lakes in late spring and summer. At times, spurious prediction of fog formation was also
223 noted on or near small lakes due to erroneous lake temperatures and resultant fluxes.

224
225 Further investigation revealed the water temperatures for small lakes used in NOAA
226 weather models were assigned via horizontal interpolation from larger, deeper bodies of
227 water (with available AVHRR data) in the design for the NOAA real-time gridded SST
228 analysis (RTG_SST_HR, Gemmill et al, 2007). An example of the analysis is shown in
229 Fig. 2. Temperature for the larger, deeper water areas has a lesser and more lagged
230 seasonal variation than the smaller, shallower lake areas due to their large heat storage
231 capacity. So use of the NOAA SST fields for lake temperatures resulted in generally
232 too-low values through spring and summer, and even into autumn. In situations with
233 atmospheric cold outbreaks in the autumn, shallow lake temperatures quickly decrease
234 (as reflected with lake cycling) and SST-based estimated lake temperatures were too
235 high. This behavior was consistent with the HRRR and RTMA deficiencies noted by
236 forecasters. In February 2020, NOAA changed from the RTG_SST_HR to a Near-
237 Surface Sea Temperature (NSST, see NWS, 2020) for SSTs, but using the same
238 horizontal interpolation method to estimate small-lake temperatures resulting in the
239 same temperature biases for small lakes.

Formatted: Header

Deleted: -

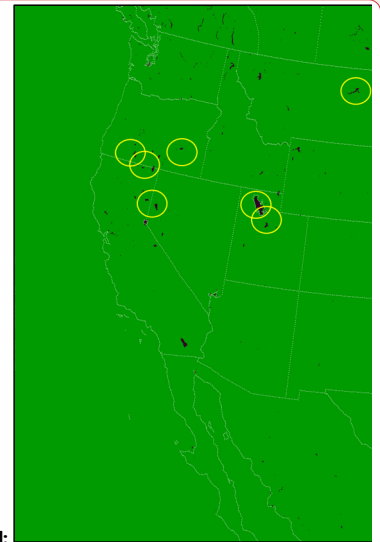
Deleted: on many occasions

Deleted: 2

Deleted: ,

Deleted:).

Deleted: -



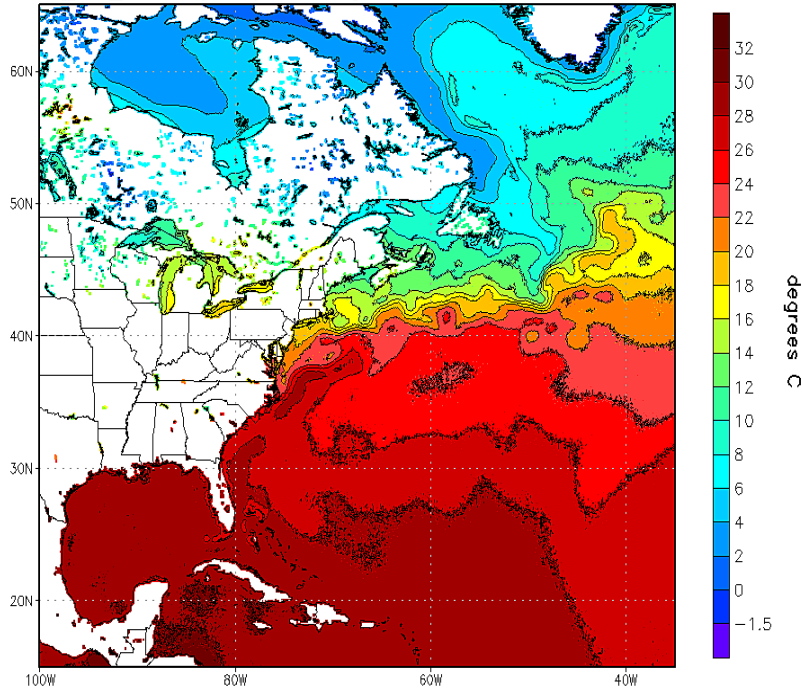
Deleted:

Fig. 2. Lakes (here, in black) circled for those with related problem reports from US National Weather Service Forecast Offices on nearby deficient 2-m air temperature or dewpoint forecasts in NOAA hourly updated models during 2004-2019.

Deleted: 3

NOAA/NWS/NCEP/EMC Marine Modeling and Analysis Branch Oper H.R.

RTG_SST_HR Analysis (0.083 deg X 0.083 deg) for 09 Oct 2019



22:40:13 WED OCT 9 2019

Fig. 2. An example of small-lake temperatures spatially interpolated from deeper-water temperature data in the NOAA SST analysis (Gemmill et al, 2007). For 9 October 2019, provided by NOAA National Weather Service.

Hamill (2020), in a comparison benchmarking a statistical method for 2 m temperature (at 00 UTC), showed the same problem with large summer temperature biases from the HRRR 1-h forecasts in August 2018 especially in the vicinity of lakes (his Figs. 10, 11). His results are shown in Fig. 3, with three stations showing coldest biases (at 00 UTC) greater than 2 K (circled in red), all adjacent to lakes. In Fig. 3, these circled stations, from north to south, are KFGN (Flag Island on Lake of the Woods; >3 K cold bias), KRRT - Warroad, MN (west of Lake of the Woods), and KVVU – Waskish, MN (east of Red Lake)). The overall warm or cold biases are generally < 2 K, but these stations adjacent to lakes are outliers, consistent with introduction of cold-biased lake temperatures through the NSST.

Formatted: Header

Deleted: 3

Deleted: -

Deleted: 4

Deleted: 4

HRRR bias, August 2018

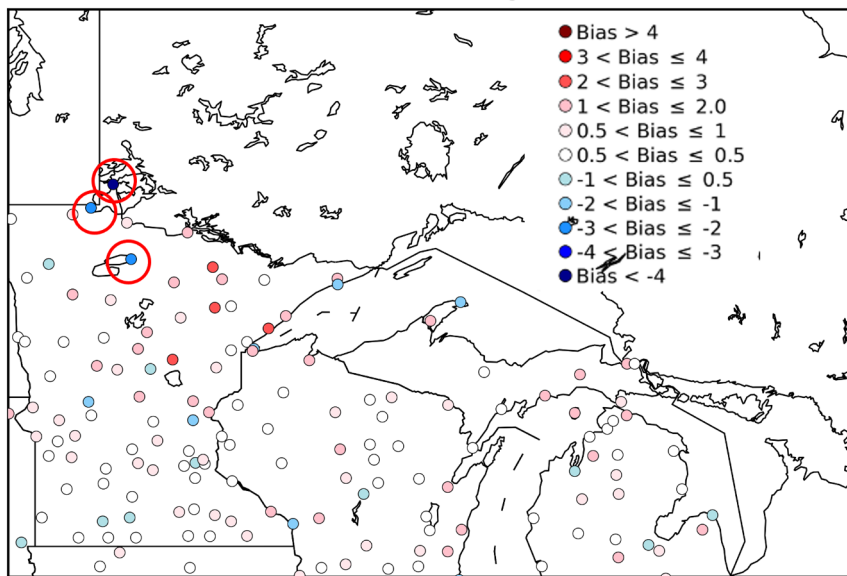


Figure 3. 2 m temperature biases for 1-h HRRR forecasts valid at 00 UTC in August 2018 (from HRRRv3, before introduction of lake cycling and using NSST estimates instead, HRRR versions and dates are listed in D22.). Stations with low bias < -2 K are circled in red. (Credit and thanks to Thomas Hamill, providing a regional version of his Fig. 10b in Hamill, 2020).

With its 3 km grid spacing, the HRRR model can resolve many inland lakes (Fig. 1). Specification of surface temperatures for these small lakes using the horizontal interpolation from the NOAA SST fields was problematic being determined by interpolation from large lake and ocean temperatures.

In summary, errors in specified lake temperatures (as well as ice cover and concentration) due to spatial interpolation from oceans and larger lakes can lead to degraded atmospheric predictions in the vicinity of lakes. For small lakes, poor short-range 2 m temperature (T) and 2 m dew point temperature (T_d) forecasts were noted in vicinity of lakes, especially from spring through summer and into autumn. Specifically, fluxes from lakes were often poorly estimated due to inaccurate lake temperature fields.

Deleted: 4

Deleted: -

Deleted:).

Deleted: -

Deleted: 1a

Deleted: -

Deleted: -

|

Formatted: Header

3 Lake model for coupling with NOAA regional atmospheric models

Similar to the now-commonplace (in NWP models) coupling with land-surface models (LSMs) to improve fluxes into the atmosphere, a multi-level 1-d lake model was implemented within the operational 3-km HRRR and 13-km RAP weather models in December 2020, an extension to atmosphere-surface coupling. An effective lake initialization is a necessary complement for the lake model coupling, as described in section 4. Different earth-system coupling processes represented in the HRRR and RAP models are described in Table 1, including land, snow, ice, and smoke. The Community Land Model (CLM) lake model (same in versions 4.5 and 5.0) was added for smaller lakes as an option in the WRF model version 3.6 (Mallard et al, 2015). The CLM lake model is described in more detail below with its configuration for the NOAA HRRR and RAP weather models. A detailed description of the physical processes (cloud microphysics, turbulent exchange, land-surface, etc.) in the HRRR and RAP models are described by [D22](#) and Benjamin et al (2016).

Deleted: Dowell et al (2022)

Component	Prognostic variables	Layers (below surface except for smoke)	Year introduced for experimental cycling	Year intro for NCEP	Data assimilation	Other information, references
Soil	Temp, moisture	9	1996 (6 levels until 2012)	1998 (6 levels until 2014)	Cycling, atmos-to-soil coupled DA	Moderately coupled DA (Benjamin et al 2022)
Snow	Water equiv, snow depth, temp	2	1997	1998	Cycling, atmos-to-snow DA for temp, trim/build from sat for cover	Moderately coupled DA . Subgrid fraction intro 2020
Ice	Temp	9	2010 (6 levels until 2012)	2012 (6 levels until 2014)	Cycling, atmos-to-surface coupled DA	Subgrid fraction intro 2018
Smoke	Smoke mixing ratio	50 atmos layers	2016	2020	Cycling, fire rad power from sat	No direct DA, only cycling
Small lakes	Temp, ice fraction, mixing	10	2018	2020	Cycling	No direct DA, only cycling
Large lakes (Great Lakes)	Temp, ice fraction, mixing	FVCOM levels	2018	2020	Independent	FVCOM driven by HRRR wind, rad, temp, 6h lag (Fujisaki-Manome et al 2020)

Table 1. Earth-system coupling added to NOAA regional models (HRRR, RAP, RUC (pre-2012))

Deleted: ¶
¶

An additional improvement in lake-atmosphere coupling in NOAA weather models for large lakes (>15,000 km²) was recently introduced, a coupling between the NOAA HRRR model using predicted lake temperatures and ice concentration fields from the NOAA GLERL/NOS 3-dimensional hydrodynamic-ice model run in real time over the Laurentian Great Lakes, as described by Fujisaki-Manome et al (2020). This hydrodynamic-ice model is based on the Finite Volume Community Ocean Model (FVCOM, Chen et al., 2006, 2013) coupled with the unstructured grid version of Los Alamos Sea Ice Model (CICE; Gao et al., 2011) and is applied to the NOAA Great Lakes Operational Forecast System (GLOFS, Anderson et al., 2018). This time-lagged data coupling (alternate applications of HRRR atmospheric forcing and FVCOM-CICE lake forcing about 6-12 h in advance) was incorporated to improve lake-effect snow (LES) predictions in winter but has also been found to improve near-lake atmospheric predictions year-round especially for upwelling events in the warm season. The use of FVCOM-CICE to specify lake temperatures addresses previous errors in SST from relatively fast changes in lake temperatures due to cold air outbreaks or upwelling

events. These changes sometimes escape AVHRR-derived SST detection due to multi-day cloud obscuration.

Small lake size (grid points)	# Lakes	% of # of small lakes	% of small lake surface coverage	Avg depth (m)	Surface area of lakes (km ²)	Volume of lakes (km ³)
1 grid point (3kmx3km)	917	49%	7%	13	8,812	115
2 (~20 km ²)	323	17%	5%	12	6,208	76
3	155	8%	4%	11	4,468	49
4-5	157	8%	6%	14	6,746	97
6-10 (~100 km ²)	155	8%	10%	14	11,570	162
11-100 (~1000 km ²)	141	7%	30%	21	35,518	769
>100	16	<1%	38%	14	44,926	614
All	1864	100%	100%		118,248	1,882

Table 2. Characteristics of small lakes (not including the five Laurentian Great Lakes) resolved in the 3-km HRRR CONUS domain over the lower 48 United States and adjacent areas of Canada and Mexico. Grid points were assigned as having a lake land use for points with at least 50% lake representation from the higher-resolution 15" MODIS land-use data.

Laurentian Great Lakes	Surface area of lakes (km ²)	Volume of lakes (km ³)
Superior	82,100	12,000
Michigan	57,800	4,920
Huron	59,600	3,540
Erie	25,670	484
Ontario	19,010	1,640

Table 3. Characteristics of the five Laurentian Great Lakes (surface area, volume) (Hunter et al 2015).

3.1 CLM lake model applied to HRRR for smaller inland lakes

Deleted: ¶

Subin et al (2012) describe the 1-d CLM lake model as applied within the Community Earth System Model (CESM) as a component of the overall CESM CLM (Lawrence et al 2019). Gu et al (2015) describe the introduction of the CLM lake model into the WRF model and initial experiments using its 1-d solution for both Lakes Superior (average depth of 147 m) and Erie (average depth of 19 m). The CLM lake model divides the vertical lake profile into 10 layers driven by wind-driven eddies. The atmospheric inputs into the model are temperature, water vapor, horizontal wind components from the lowest atmospheric level and short-wave and longwave radiative fluxes (from the HRRR model in this application). The CLM lake model then provides latent heat and sensible heat fluxes back to the HRRR. The CLM lake model is called every 20 s within the HRRR model. The CLM lake model was configured with the top layer fixed to a 10-cm thickness (Gu et al 2015) and with the rest of the lake depth divided evenly into the other 9 layers. Energy transfer (heat and kinetic energy) occurs between lake layers via eddy and molecular diffusion as a function of the vertical temperature gradient. The version of the CLM lake model used for HRRR and RAP was introduced with CLM version 4.5 and continues without change in CLM version 5 (Lawrence et al, 2019). The CLM lake model also uses a 10-layer soil model beneath the lake, a multi-layer ice formation model and up to 5-layer snow-on-ice model (Gu et al, 2015). Testing of the CLM lake model by the authors within WRF showed computational efficiency of the model with no change of even 0.1% in run time with the HRRR and RAP applications. Multiple layers in lake models better represent vertical mixing processes in the lake. By intention, the CLM lake model was only applied for HRRR and RAP model to smaller lakes, since NOAA began at the same time to provide temperature and ice cover through GLOFS for the Laurentian Great Lakes through the 3-d hydrodynamic-ice model (Fujisaki-Manome et al, 2020, Anderson et al, 2018).

3.2 Lake area mask

Grid points were assigned as lake points when the fraction of lake coverage in the grid cell (derived from yet finer 15" MODIS data) exceeds 50% and when HRRR gridpoint elevation > 5 m above sea level (ASL, to distinguish from ocean) and is disconnected from ocean areas with the 3-km land-water mask. The lake water mask is therefore binary, set to either 1 or 0. This binary approach at 3 km seemed capable of capturing the effect of lakes on regional heat and moisture fluxes. The alternative subgrid lake fraction approach was used by ECMWF with their 9-km model (Choulga et al, 2019).

An overview of the lake number, areal coverage, and integrated volume for the 3-km HRRR model are depicted in Table 2. The HRRR CONUS domain (Fig. 1) is able to represent 1864 separate lakes occupying 0.6% of the entire domain. These water bodies represented in HRRR as "lakes" include reservoirs and larger rivers, and about half of the 1864 lakes are single-gridpoint lakes. The sixteen largest lakes in the HRRR CONUS domain have surface area greater than 1,000 km², nine in Canada and two on the US-Canada border (Lake of the Woods and Lake St. Clair). In contrast, the five

Deleted:).

Deleted: 1a

Laurentian Great Lakes (Table 3) range in size from 82,000 km² (Superior) to 19,000 km² (Ontario), and therefore, their representation in the coupled HRRR system (Table 1) is handled with 3-d hydrodynamic-ice models (Fujisaki-Manome et al, 2020).

The lake area mask for the 3-km HRRR used an algorithm for identifying an ocean area mask for all areas with contiguous water areas and leaving other areas **also below 5 m ASL** as near-ocean lagoon regions treated as lakes with the CLM 1-d lake model. These lagoon areas separated from ocean by barrier islands in the HRRR representation (Fig. 1) include the Intracoastal Waterway in Texas largely separated from the Gulf of Mexico by Padre Island, Indian River in Florida largely separated from the Atlantic Ocean by Merritt Island, and Lake Pontchartrain in Louisiana. This ocean-contiguity technique is similar to the flood-filling technique used by ECMWF (Choulga et al, 2019).

3.3. Lake depths

Lake depths for the HRRRv4-WRF-CLM lake configuration are assigned from a global dataset provided by Kourzeneva et al (2012b, hereafter K12). For some smaller lakes identified using the 15" MODIS land-water mask not found in K12, a 50 m depth was assumed (**too deep, will be reduced in future**). **K12 identified uncertainties in their own database including estimates of lake depth and errors in coastlines**. ECMWF applied a 25 m depth as a default depth for these small lakes (Choulga et al, 2019). For many lakes in the K12 database, a single value for maximum lake depth had been applied to all lake points, which results in excessive lake water volume and too cold temperatures as discussed in section 5. However, the K12 database still allows overall differentiation between shallow and deep lakes. The majority of the small lakes in the northern US and southern Canada are assigned as shallow, at 5 m depth, but a few are assigned a depth as 30 m or deeper (Fig. 4).

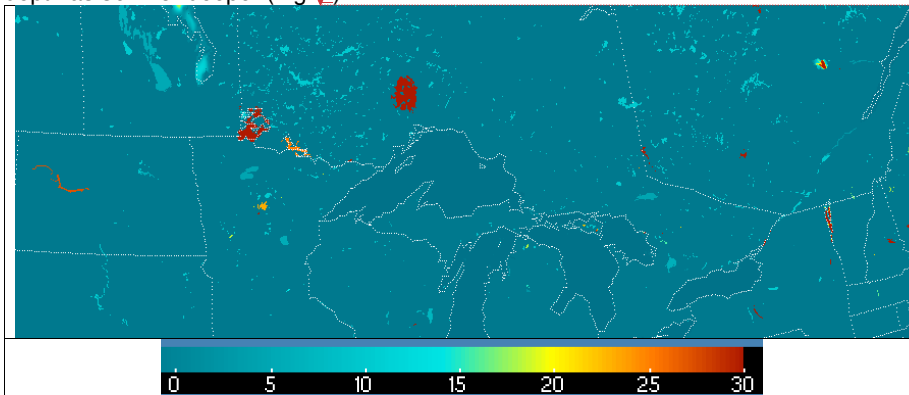


Figure 4. Lake depth for small lakes in a subset of the HRRR domain with red for lakes 30 m or deeper.

Formatted: Header

Deleted: 1a

Deleted: ¶

Deleted: 2012

Deleted: -

Deleted: .

Deleted: -

Deleted: -

Deleted: 5

Deleted: 5

3.4 Turbidity

A single value for turbidity to describe absorption of downward short-wave radiation is used in CLM, allowing for a moderate amount of suspended sedimentation. Subin et al (2012) describe other options for variations in radiative transfer in lake bodies to capture degrees of eutrophication, but these are not used here.

3.5 Salinity

The CLM lake model is configured for fresh water. The authors manually modified the freezing temperature to account for non-zero salinity (Railsback, 2006) from 0°C to -5°C for Mono Lake in California and Great Salt Lake (GSL) in Utah to capture the effect of salinity. Other areas of water impoundment from coastal lagoons in the 3-km HRRR lake representation (Fig. 1) also have, ~~in reality~~, non-zero salinity (e.g., along coasts of Gulf of Mexico and Atlantic Ocean) but ~~this is not applied in HRRR/RAP. Moreover~~, no change in freezing temperature is necessary for these areas ~~anyway~~.

Deleted: 1a

3.6 Elevation

The elevation value (above sea level) assigned to each lake grid point is the same assigned to that from the atmospheric model, which may be different from reality, but at least consistent with the atmospheric conditions. As mentioned earlier, the minimum elevation above sea level of a grid point to be assigned as a lake is 5 m; other water grid points are assumed to be ocean.

3.7 Special situations for CLM lake model application

The algorithm for the turbulent heat flux calculation in the CLM-lake model was mainly based on Zenget al. (1998), except that roughness length scales for temperature and humidity are the same as roughness length scale for momentum for its WRF-lake application, while they are updated dynamically in CLM 4.5. Charusombat et al (2018) showed that the same roughness length scales for temperature and salinity as that for momentum could result in overestimated surface sensible and latent heat fluxes in autumn and winter. Therefore, a revision to the CLMv4.5 lake model was introduced for modified roughness lengths over water using modified formulations of the Coupled Ocean-Atmosphere Response Experiment (COARE) algorithm as described by Charusombat et al (2018) to improve surface sensible and latent heat fluxes.

For GSL with a very high value of salinity (270 ppt north of ~41.22°N with freezing point of 249 K and 150 ppt south of ~41.22°N with freezing point at 263 K), a change of freezing temperature to -5°C appeared to be not sufficient to keep the lake ice-free during the cold outbreaks in winter in this high-elevation area. GSL is unusual in various aspects – it is hypersaline (far more saline than the ocean), the largest terminal lake

Formatted: Header

(without outflow) in the Western Hemisphere (Belovsky et al, 2011), shallow (mean depth of 5 m) and subject to very strong eutrophication (Belovsky et al, 2011). According to GSL climatology the lake stays ice-free all winter, and its temperature goes slightly below freezing only for a very short period in January and February. Thus, we presume that the CLM lake model needs to allow turbidity variation (see section 3.4). A solution to this representation problem was use of a bi-weekly climatology over each 1-year period to bound the cycled GSL temperature at initial forecast time not to deviate more than +/- 3°C from the climatological value interpolated to the current day of year. Also, using special code, GSL was forced stay ice-free for the whole year as observed.

3.8 Time step

The CLM lake model within the HRRR/RAP weather models was run with the same time step as for other physical processes in the HRRR model (20 s) and the RAP model (60 s). Again, even with this relatively high frequency for calling the CLM lake model, the computational expense was extremely small, less than 0.1% of overall HRRR run time.

4 Initialization for small lake temps by cycling with ongoing atmospheric predictions – a strategy

The central strategy described in this paper is to use accurate, ongoing atmospheric forcing with a computationally inexpensive 1-d lake model to obtain an equilibrium state of a lake temperature profile. This technique responds appropriately to strong changes in atmospheric forcing (e.g., cold air outbreak or excessive heat events). With the NOAA HRRR and RAP atmospheric models performing hourly data assimilation of a broad set of hourly observations, accurate atmospheric forcing is available.

The RAP and HRRR hourly data assimilation cycles include these aspects, all of which are important for cycling initialization of inland lakes. First, cloud assimilation (from satellite and ceilometer data) to ensure accurate shortwave and longwave radiation fields (Benjamin et al 2021). Second, radar reflectivity data are assimilated as part of a 3-km ensemble data assimilation system to ensure accurate short-range precipitation (Weygandt et al, 2022, D22, J22, Benjamin et al, 2016). Finally, 2 m air temperature and moisture and 10 m wind observations are effectively assimilated (i.e., producing more accurate predictions) including representation through the boundary layer using pseudo-innovations (James and Benjamin, 2017, meaning estimated observation-background forecast differences but not actual). Other information on the HRRR/RAP data assimilation is provided by Benjamin et al (2016) and D22.

The cycling of the 10-level CLM lake model within the experimental HRRRv4 started on 24 August 2018. After 10 days of cycling (Fig. 4), differences in lake temperatures between HRRRv4 and the operational HRRRv3 using interpolated NSST data were

Deleted: defined

Deleted: conditions

Deleted: Dowell et al, 2022, James et al, 2022

Deleted: -

Deleted: -

Deleted:).

Deleted:).

Deleted: 5

evident of 5-15°F (3-12°C or 276-285 K), showing that the adjustment with realistic atmospheric conditions and use of the CLM lake model with roughly accurate lake depth data was very effective.

Consequences (to right) from strategy for lake initialization (below)	Coupling lake and atmosphere within initialization	Lake temps in spring-summer	Lake temps in fall
SST interpolation to small lakes	None	Much too cold, especially for shallow lakes	Still generally too cold but intermittently too warm after cold-air outbreaks.
Lake annual variation forced by reanalysis atmospheric data – 1-way cycling from atmospheric forcing	1-way	More accurate. No weather regime variation in a given year	More accurate. Will not capture variation from weather regimes in a given year.
Daily updating with satellite data	None	More accurate but cannot keep up with changes during cloudy periods.	More accurate but cannot keep up with changes during cloudy periods.
2-way coupled cycling	2-way	More accurate including response to specific yearly/seasonal anomalies.	More accurate including yearly/seasonal anomalies

Table 4. Expected seasonal lake-atmosphere temperature consequences from different lake initialization strategies

Possible approaches for initializing lake temperatures are summarized in Table 4. The simplest option is via larger-scale water temperature data (SST data) with horizontal interpolation to smaller water areas including inland lakes and reservoirs; this was the previous strategy for the HRRR and RAP models before introduction of cycling using the CLM lake model. An alternate strategy is to run lake models over a multi-year period forced by reanalysis atmospheric data (ERA-Interim) as described by Balsamo et al (2012), Dutra et al (2010), and Balsamo (2013) for the ECMWF to obtain a yearly varying climatology of lake temperature for all lakes represented. This method will capture the mean annual variation of lake temperatures. However, due to multi-year averaging, it cannot represent anomalous conditions in a given year (sustained heat or sustained cold conditions), which can modify temperatures especially for shallow lakes by several K within 1-2 weeks. Use of daily updating from satellite data can be effective (e.g., MetOffice – Fiedler et al, 2014) under clear-sky conditions. Full cycling of the lake model within an ongoing coupled weather model, the strategy described in this paper,

Formatted: Header

Formatted Table

Deleted: , possibly still too cold.

Deleted: , still too cold for some lakes with too-deep bathymetry data.

Formatted Table

can represent the lingering effects of anomalously warm or cold weather upon lake temperatures and the resultant fluxes.

The 2-way coupled cycling (Table 4) used now in the HRRR and RAP models benefit via hourly data assimilation using latest hourly observations both for the atmosphere (D22) and land-surface snow conditions (Benjamin et al 2021). In the 3-km HRRR model, the 3-d state of the atmosphere, land surface, and inland lake conditions are advanced on 20-second time steps using the HRRR-specific configuration (described in D22) of the WRF model (Powers et al, 2017; Mallard et al, 2015). As atmospheric conditions change every 20 s (including temperature, moisture, wind, and radiation), the exchange of heat, moisture, and momentum between inland lake points and the atmosphere also vary. Lake temperature is not modified in the hourly data assimilation step, but the ongoing exchange recalculated every 20 s forces an evolution of lake conditions to values consistent with atmospheric conditions. ECMWF applies a similar ongoing cycling for lake prognostic variables (ECMWF, 2020) for lake initialization.

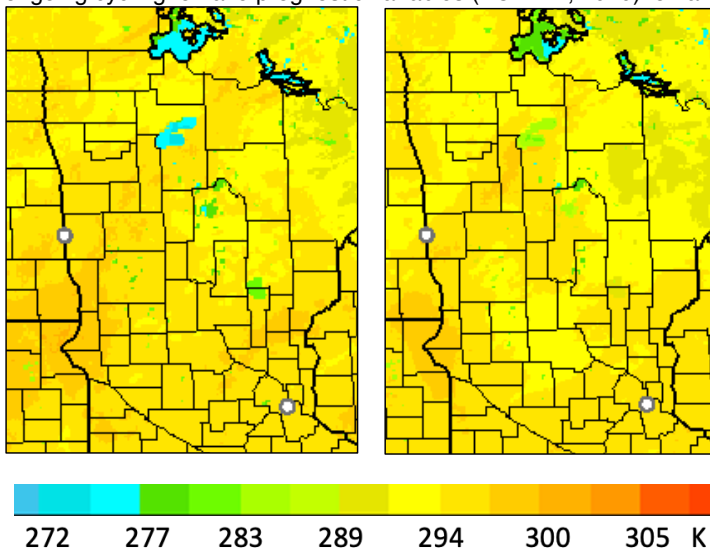


Figure 5. Skin temperature (K) including lake temperatures. From 18-h forecasts valid at 15 UTC 3 September 2018 for a) operational HRRRv3 using NSST for lake temperatures, and b) then-experimental HRRRv4 with CLM lake model and cycling.

A similar challenge is initialization of lake ice cover. Similar to the treatment for lake temperature, cycling of a multi-level lake model (like the CLM lake model) can provide an alternative, adaptive-in-time method for lake-ice initialization. NOAA has used in the

HRRR and RAP the daily IMS ice cover product¹ (US National Ice Center, 2008) for binary (non-fractional) lake ice cover. The IMS ice cover is used for oceans and large lakes (e.g., for RAP for Great Slave Lake and Great Bear Lake in northern Canada). For small lakes below the resolution of the IMS ice map, lakes stayed open for the winter. Starting with HRRRv4 and RAPv5, ice concentration from the NOAA global model is used for oceans, FVCOM ice fraction is used for the Great Lakes, and ice fraction from the CLM lake model for small lakes.

5 Results

In this section, we describe comparisons of lake surface temperature evolution between the CLM implementation described here and the lake specification through interpolation from the NSST dataset (Fig. 2) at lakes in the United States and southern Canada.

Comparisons during 2018–2019 were drawn from real-time simulations from the then-operational HRRRv3 (using interpolated SST) and the experimental HRRRv4 (using CLM). More recent comparisons were made for March–November 2021 between the operational HRRRv4 (using CLM) and interpolated NSST values (as used in 2019–2020 for HRRRv3). In addition, the CLM and NSST values were compared to in situ observations where available and also to satellite-based estimates defined below.

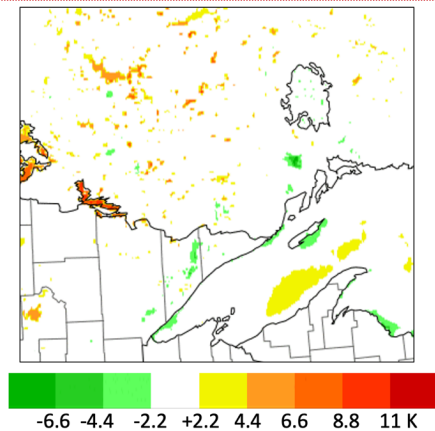


Figure 6. Difference (K) in skin temperature (including lake temperatures) between versions of HRRR model using cycled lake-model values (HRRRv4 or HRRRX) and using interpolated NSST data (HRRRv3 or HRRR-NCEP). Valid 1300 UTC 13 October

¹ <https://usicecenter.gov/Products/ImsHome>

Formatted: Header

Deleted: in Fig. 1b,

Deleted: before introduction of the CLM lake model with lake cycling (for grid-point-specific temperature and ice cover) starting with HRRRv4 and RAPv5.

Deleted: ¶

Deleted: 3

Deleted: ¶
¶

Deleted: Fig. 7

2019, and also includes differences from use of FVCOM lake model in HRRRv4 (Fujisaki-Manome et al, 2020).

5.1 Cases from 2018 – 2019

Introduction of the CLM lake model forced by ongoing HRRRv4 atmospheric conditions (i.e., cycling) allowed, within only 10 days, an increase in lake temperatures for Red Lake and Lake of the Woods (both in Minnesota) from 3 K to over 10 K (Fig. 5) in September 2018. A comparison in skin temperature for a year later (October 2019) between versions of the HRRR model (HRRRv4 with lake cycling vs. HRRRv3) including differences from with and without lake cycling is shown in Fig. 6. Higher temperatures were evident for the Minnesota/Ontario lakes from cycling (vs. NSST interpolation). HRRRv4 also included coupling with the 3-d FVCOM lake model for the Laurentian Great Lakes, showing areas of upwelling with associated cooler water over Lake Superior in Fig. 6 from predominant westerly to southwesterly near-surface wind at this time.

Deleted: 6

Deleted: 7

Deleted: 7

Lake number	Lake name	State/province, country	HRRR l point	HRRR j point	Area (km ²)	Depth used (m)	Ice free?
1	Simcoe	ON, CA	1378	799		6	N
2	St. Clair	ON/MI, CA/US	1302	709	1240	6	N
3	Champlain	VT/NY, US	1534	835		77	N
4	Sebago	ME, US	1610	833		33	N
5	Okefenokee	FL, US	1459	145	1510	3	Yes
6	Pontchartrain	LA, US	1136	224	2180	10	Yes
7	Intracoastal Waterway (near Corpus Christi, TX)	TX, US	905	128	3300	10	Yes
8	Salton Sea	CA, US	337	387		9	Yes
9	Tahoe	NV/CA, US	259	628		313	N
10	Great Salt	UT, US	486	653	3050	3	Yes
11	Utah	UT, US	496	622		3	N
12	Bear	ID/UT, US	518	684		29	N
13	Sakakawea	ND, US	790	868		27	N
14	Winnebago	WI, US	1143	742		7	N
15	Lower Red	MN, US	961	880		5	N
16	Lake of the Woods	MB/MN, CA/US	965	919	3030	32	N
17	Manitoba	MB, CA	879	972	3240	5	N
18	Winnipeg	MB, CA	916	977	13270	8	N
19	Nipigon	ON, CA	956	956	5410	55	N

644 Table 5. Lakes for comparison of lake temperatures between HRRR/CLM, NASA
645 SPoRT, NSST, and in situ observations as shown in Figs. 7 and 8. Area is shown for
646 lakes >1000 km². Lake depths are constant within each lake except for lakes 2, 3, and
647 18. See Fig. 4 for example map of lake depth used in HRRR. Specific HRRR i/j 3-km
648 grid points (indicated in table) were selected from HRRR data for each lake.
649

Formatted: Header

Deleted: 8

Deleted: 9

Deleted: 5

Name of Lake	No. from Tab. 5	Source of Observation	Depth of Sensor (m)	URL
Lake St. Clair	2	ECCC	6	https://www.ndbc.noaa.gov/station_page.php?station=45147
Lake Champlain - Schuyler Reef	3	GLERL	0.45	https://www.ndbc.noaa.gov/station_page.php?station=45195
Sebago Lake @ Lower	4	Portland Water District Buoy	Est 1	https://www.pwd.org/sebago-lake-monitoring-buoy
Lake Pontchartrain @ New Canal Station	6	NOAA/ National Ocean Service	0.6	https://www.ndbc.noaa.gov/station_page.php?station=nwcl1
Intracoastal Waterway @ Baffin Bay near Padre Island	7	Texas Coastal Ocean Observing Network	unknown	https://www.ndbc.noaa.gov/station_page.php?station=babt2
Lake Tahoe	9	NASA/JPL	0.5	https://laketahoe.jpl.nasa.gov/get_imp_weather
Utah Lake @ Provo Marina	11	Utah DWQ Water Quality Network	unknown	https://wqdatalive.com/public/669
Bear Lake	12	Utah DNR State Parks	unknown	https://stateparks.utah.gov/parks/bear-lake/current-conditions/
Lake Sakakawea @ Missouri River near Williston, ND	13	USGS	unknown	https://waterdata.usgs.gov/monitoring-location/06330000/#parameterCode=00065&period=P7D

Table 6. Sources of available in situ data among 19 lakes in Table 5.

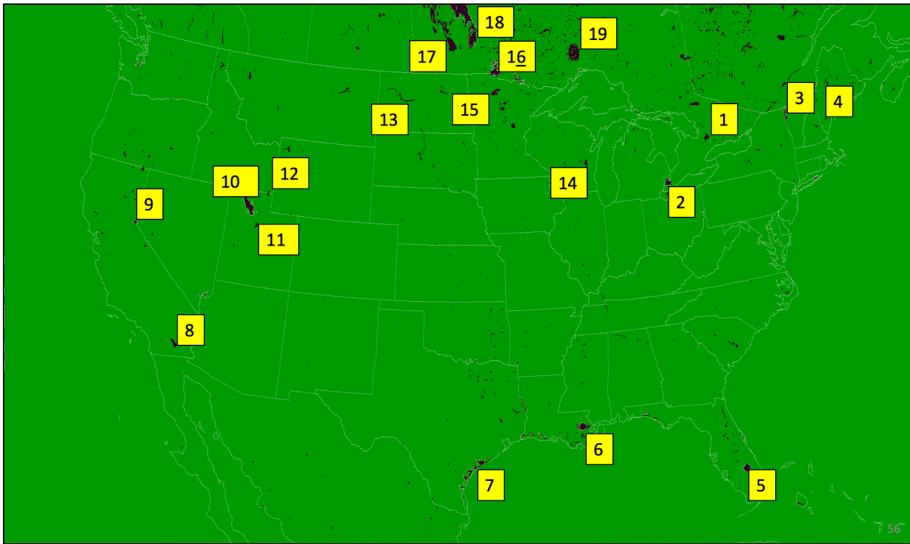


Figure 7. Locations of 19 lakes (see Table 5) for lake temperature intercomparison. These lakes are shown as mapped onto the 3-km CONUS HRRR model domain.

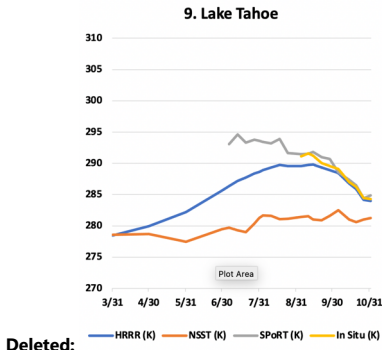
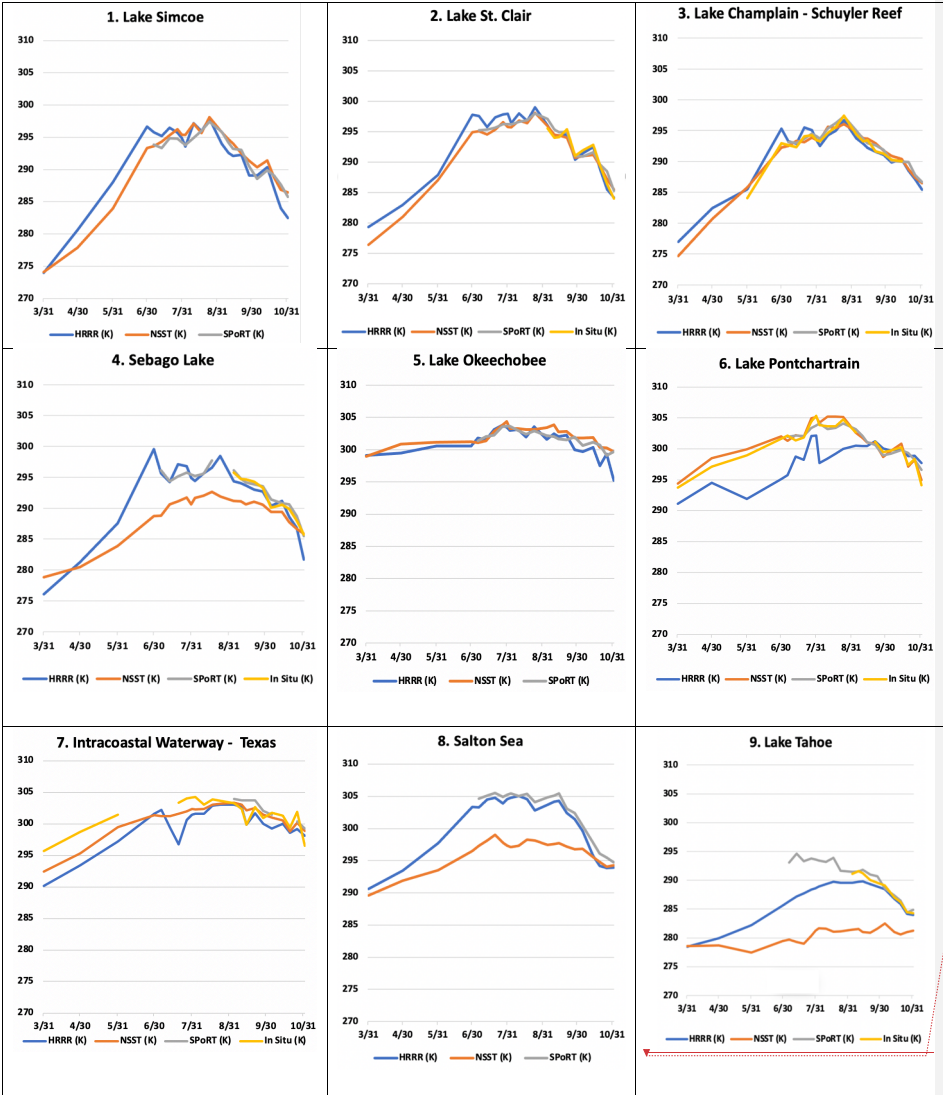
Deleted: 8

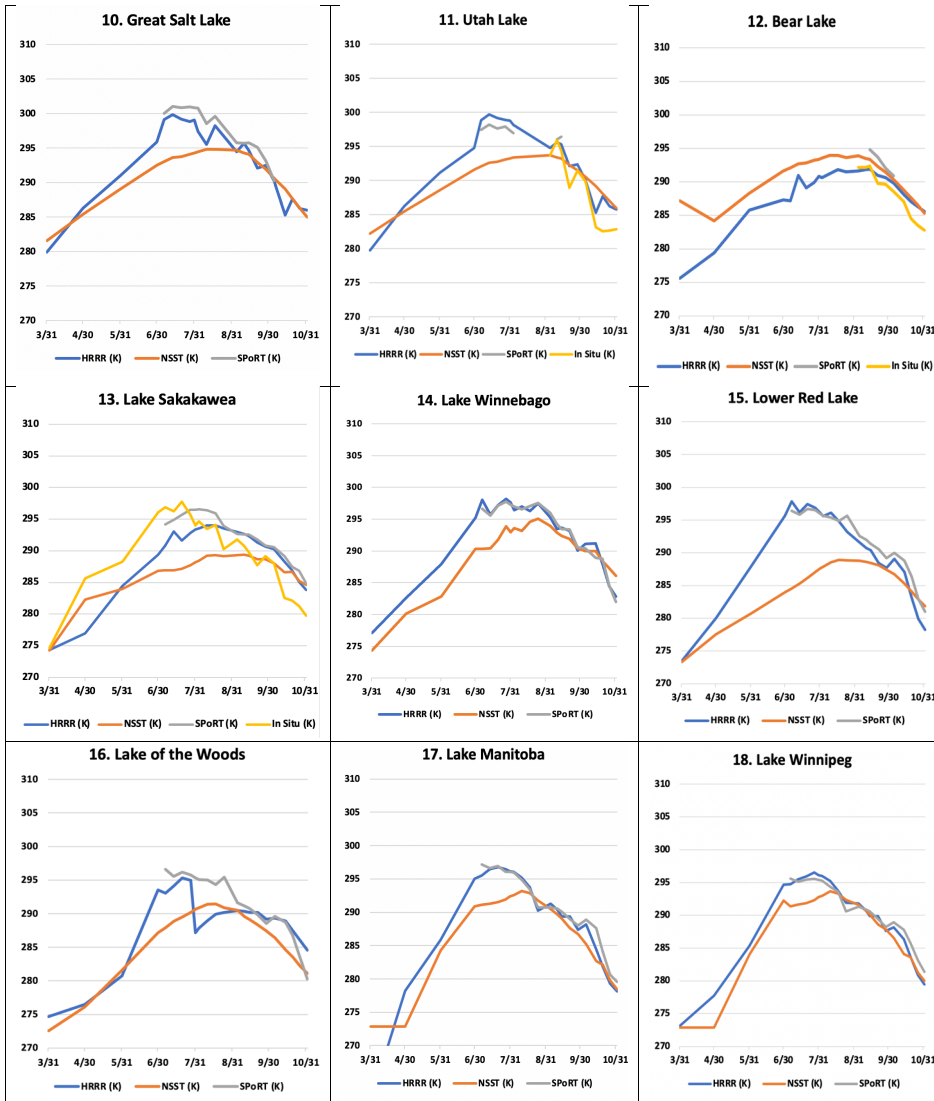
5.2 Comparisons of different lake temperature estimates for 19 lakes from lower 48 US and southern Canada during 2021.

During a period from March to November 2021, a comparison was made of lake temperatures between the cycled HRRR-CLM values and those from three other estimates from NASA, NOAA, and in situ observations. A geographically diverse set of 19 lakes over the lower 48 United States and southern Canada was selected for these comparisons as listed in Table 5 and shown in Fig. 7. Lakes selected included near-ocean lagoon areas separated from ocean areas by coastal land as resolved by the 3-km land-water mask as discussed in section 3.2. The water areas also included a reservoir (Lake Sakakawea). Some of these lakes are dimictic or polymictic (with ice cover part of each year, Lewis 1983) but five of them do not experience any ice cover (Table 5), and lakes 5, 6, 7, and 8 are monomictic. The CLM lake model was cycled for all these lakes in the 3-km HRRR model. The 19 lakes included seven lakes with a surface area greater than 1,000 km². The March-November evaluation period include the spring-summer warming period and the cooling period in autumn. Data points were obtained monthly for March-August and weekly for September-November.

Deleted: 8

Formatted: Header





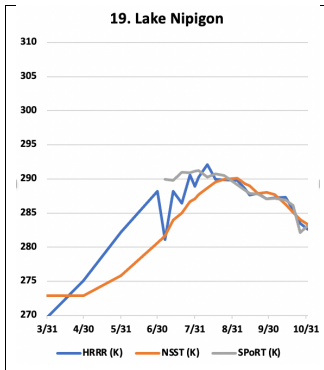


Figure 8. Lake temperatures in 2021 (April–October) from the 19 selected lakes (Table 5, Fig. 7) from HRRR-CLM-cycled (blue), NSST (red), SPoRT (gray), in situ (orange).

The HRRR-CLM values for these 19 lakes were compared with first, an estimate from NASA SPoRT (Short-Term Prediction Research and Transition) real-time surface water temperature composite including time-weighted MODIS and VIIRS data for inland lakes (NASA, 2021, Kelley et al, 2021). The SPoRT estimates are similar to the satellite-based lake temperature estimates from the Met Office (Fiedler et al 2014). The SPoRT composite is valid from the surface to 2 m depth and is averaged over a 7-day period to mitigate for cloud cover on a given day. A second lake temperature estimate is that from NSST, as discussed earlier. Third, in situ surface water temperature observations were available from observing platforms in nine of the 19 lakes (Table 6). The platforms are operated by Federal, state, and local government agencies and a regional ocean observing system. The depths of the water temperature observations were only available at four of the nine platforms. At these four sites, the depth ranged from 0.45 to 0.9 m.

In general, the HRRR-CLM-cycled lake temperatures showed the anticipated difference from NSST values with quicker summer warming from HRRR-CLM cycling for all lakes except the southern 3 lakes (5, 6, 7 in Table 5, with Lakes 6 and 7 essentially lagoons in close proximity to the ocean) and Bear Lake in UT/ID (Lake 12, 39 m depth). The NSST estimates were colder for spring through summer than HRRR values for 15 of the 19 lakes, a consequence from the NSST estimate via horizontal interpolation from deeper bodies of water.

For the nine lakes with in situ observations (Table 6), the HRRR-CLM-cycled lake temperatures are generally able to better capture weekly variability in summer and autumn months, associated with windy periods increasing mixing or relatively warm and cool weather periods or varying amounts of cloud cover. This can be seen, for

Formatted: Header

Deleted: 9

Deleted: 8

Deleted: The

Deleted: -

Deleted: -

|

Formatted: Header

723 example, at Utah Lake and the Intracoastal Waterway west of Padre Island in Texas
724 (note cooling from passage of Hurricane Nicholas in mid-September). The most
725 dramatic improvement of HRRR-CLM over NSST lake temperatures is seen at Lake
726 Tahoe and lakes 14-19 in the northern region, with NSST estimates 5-10 K too cool. At
727 two of the lakes with in situ observations, the Intracoastal Waterway (linked to the
728 ocean) and Lake Pontchartrain, both lagoons linked to the ocean, NSST estimates are
729 generally closer than HRRR-CLM to the observations.

731 HRRR-CLM lake temperatures matched in situ observations well for the northern lakes,
732 usually within 1-2 K. In contrast, the lake temperature values from SPoRT were
733 generally warmer than HRRR or in situ observations in the autumn period. The SPoRT
734 observations showed a strong confirmation of HRRR-CLM-cycled lake temperatures for
735 lakes in the western US (Lakes 8-13) and most lakes in the northern areas (Lakes 4,
736 14-19). Finally, the HRRR-CLM-cycled lake temperatures during this period often
737 varied strongly from the NSST estimates, with differences of up to 5-10 K (largest
738 difference with Red Lake, Lake 15). The effect of lake depth was evident with a faster
739 transition to fully mixed lakes for shallow lakes (e.g., 5 m depth for Red Lake in MN,
740 Lake 15 in Table 5) but subject to more temporal and horizontal variation for deeper
741 lakes. Fig. 9 showed a strong intralake variation of 9 K across Lake of the Woods (32
742 m depth) in the HRRR-CLM estimate in contrast with very little variation (< 1 K) across
743 Red Lake. Due to a lack of high-resolution observations of lake surface temperatures, it
744 is difficult to determine which intralake variations are more realistic. However, we think
745 some of these intralake contrasts from HRRR-CLM may be exaggerated from actual
746 values, possibly requiring introduction of a small temperature exchange rate (diffusion)
747 between adjacent lake columns. Differences in skin temperature (e.g., SPoRT) and
748 bulk temperature (e.g., in situ) for lakes have been noted (e.g., Wilson et al, 2013) of up
749 to 0.5 K, but the HRRR vs. NSST differences in this study are generally much larger
750 than this magnitude.

751

Deleted: -

Deleted: 10

Deleted: -

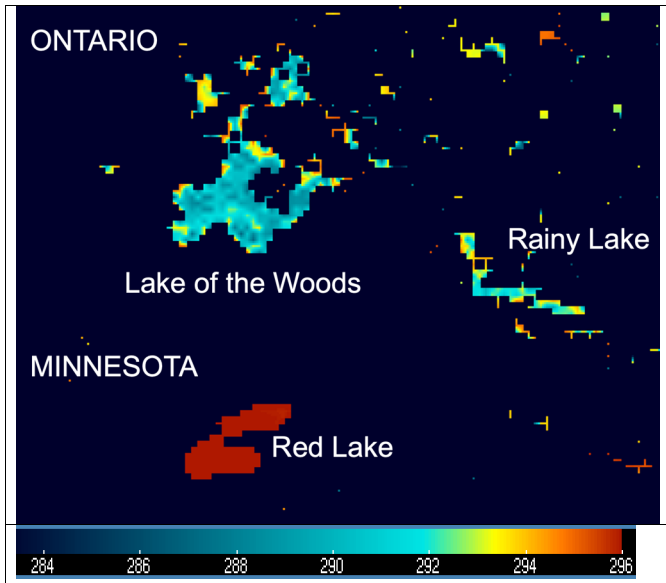


Fig. 9. HRRR-CLM lake temperature (K) for 1500 UTC 31 July 2021 for area over northern Minnesota (US) and southwestern Ontario (Canada).

The main deficiencies evident so far with the HRRR-CLM lake temperatures appear to be associated with errors in lake depth values. On the average, the **current specified values for mean** lake depth for most lakes **are** too deep **compared to reality**, since the preprocessing with the K12 dataset simply assigned a single lake depth value (maximum or mean) to all grid points for that lake even up to the modeled lake points adjacent to land, as shown in Table 5 for 16 or the 19 lakes studied. We also noted too-low lake temperatures in HRRRv4 for lake grid points at the western edge of a few lakes (e.g., Tahoe, Sebago (ME), Cayuga (NY), Champlain), all relatively deep lakes (Fig. 5, Table 5). We attribute this to 1-d upwelling from insufficient bathymetry data resulting in cylinder-like lake volumes with constant lake depths, therefore with a) too-deep lake-edge pixels coinciding with b) strong winds coming off from land areas with predominantly westerly winds. This deficient effect was not widespread for the HRRR model and did not affect the overall results. Again, this behavior is attributed to the behavior of the lake model over integrations with the inaccurate lake depth information and not to the lake cycling initialization design.

6 Conclusions

Formatted: Header

Deleted: 10

Deleted: is

Deleted: 6

We report here on the first use of a small-lake model (CLM4.5, 10 layer) in US NOAA NWP models along with an ongoing cycling of lake temperatures since 2018 to initialize lake temperatures in each prediction. These models are the 3-km HRRRv4 (D22, J22) and 13-km RAPv5 hourly updated models, both of which became operational in December 2020 after cycling since August 2018. At 3-km grid spacing, the HRRR model applied this small-lake modeling and assimilation to 1864 small lakes varying in size from about 10 km² (single grid point) to 14 larger lakes over 1000 km² in surface area, but not including the Laurentian Great Lakes. The effectiveness of introducing the multi-layer lake model into the HRRR and RAP models was completely dependent on the initialization for lake temperatures. The introduction of a cycling capability through the hourly assimilation allowed the lake temperatures to evolve to accurate values, consistent with recent weather. In this paper, we describe the lake cycling applied for the NOAA regional 3-km HRRR and 13-km RAP weather models including the coupled 1-d CLM lake model. We also show some comparisons with other estimates of lake temperatures. From those comparisons, the cycled lake temperatures from the 3-km HRRR model were found to be reasonably accurate. HRRR lake temperatures were found to be generally within 1 K of in situ observations and within 2 K of the SPoRT estimates. Finally, NSST estimates of small-lake temperatures were found to often differ from in situ observations and HRRR estimates by 5-12 K. Other differences between lake-cycled HRRR estimates and SST-based estimates were up to 10-15 K.

From these initial results, we conclude that the lake-cycling initialization for small lakes has been effective overall, owing to accurate hourly estimates of near-surface temperature, moisture and winds, and shortwave and longwave estimates provided to the 1-d CLM lake model every time step (20 s for 3-km HRRR model). The HRRR-CLM treatment also allows some inland lakes to freeze in winter, which is more consistent with observations. The lake cycling strategy is similar to that initialization method used by ECMWF for its 9-km (as of 2021) IFS (Integrated Forecast System) and using a binary lake mask in the 3-km HRRR model.

One deficiency noted was development of too-cold lake surface for a few lakes on their western boundary. We attribute this to the incorrect bathymetry data with constant lake depth (e.g., see caption for Table 5) causing an excessive 1-d upwelling from too-deep lake depth at western shores for these lakes. This issue is being addressed with a current project to improve lake bathymetry data for which results will be reported in the future. Also, HRRR-CLM cycling gave poorer results than NSST at least for Lake Pontchartrain (Lake #6 in Table 5), suggesting to use NSST for near-ocean lagoon areas. More investigation is needed for strong intralake variations overall in HRRR-CLM-cycling representation (e.g., Lake of the Woods in Fig. 9) and possible introduction of horizontal diffusion of temperature between adjacent lake points.

US NWS forecasters have reported much improved near-surface temperature and dewpoint predictions in the vicinity of small lakes from the 3-km HRRR model in 2021 since the implementation of the 1-d CLM lake model and lake-cycling initialization.

Deleted: due

Deleted: 10

827 Again, this effort complements the coupling of the HRRR model with the 3-d FVCOM
828 hydrodynamical lake model for the Laurentian Great Lakes (Fukisaki-Manome et al,
829 2020) design to improve lake-effect snow predictions. These efforts are the most
830 advanced lake-coupling and lake-initialization efforts at this point in US NOAA weather
831 models.

832
833 Overall, the improved lake temperatures from the lake cycling initialization technique
834 driven over a 3-year period by accurate atmospheric conditions described here results
835 in improved fluxes of heat and moisture over using SST interpolation and improved
836 nearby predictions of atmospheric 2 m temperature and 2 m moisture.

837 **Code availability**

838 This research used WRF version 3.9.1 including use of the option with the CLM lake
839 model. All code is available from the National Center for Atmospheric Research
840 (NCAR) at https://www2.mmm.ucar.edu/wrf/users/download/get_sources.html

841 **Data availability**

842 HRRR data (including lake surface temperature data under ‘skin temperature’ field) are
843 publicly available via archives hosted by Amazon Web Services
844 (<https://registry.opendata.aws/noaa-hrrr-pds/>) and Google Cloud Platform
845 (<https://console.cloud.google.com/marketplace/product/noaa-public/hrrr?project=python-232920&pli=1>).
846

847 **Author contributions**

848 SB, TS, and EJ planned the design. TS and EJ carried out the actual coding for
849 modeling, data assimilation and scripts. EJ, SB, JK, and SK extracted data from
850 experiments and other sources. EJ and JK analyzed the results. SB wrote the
851 manuscript draft and led its revision. EA, AFM, JK, GM, AG and PC (along with TS and
852 EJ) reviewed and edited the manuscript.

853 **Acknowledgments**

854 Credit is due to the WRF model team at NCAR (Jimmy Dudhia) for their help in applying
855 the CLM lake model for the HRRR and RAP applications of the WRF model. We
856 greatly appreciate our NOAA colleague, Thomas Hamill (NOAA PSL), for Fig. 3 from
857 another already published article by him. We also thank Frank J. LaFontaine and Kevin
858 K. Fuell of the NASA SPoRT Team for providing archived Northern Hemisphere SST
859 composites. Thanks also to Rob Cifelli of NOAA/PSL for a very helpful review of our
860 manuscript. This work was supported by NOAA Research base funding.

861 **References**

862 Anderson, E. J., Fujisaki-Manome, A., Kessler, J., Lang, G. A., Chu, P. Y., Kelley, J. G.
863 W., et al.: Ice forecasting in the next-generation Great Lakes Operational Forecast
864 System (GLOFS). *Journal of Marine Science and Engineering*, 6(123),
865 <https://doi.org/10.3390/jmse6040123>, 2018

Formatted: Header

Deleted: -

Deleted: -

Deleted: 4

869 Balsamo, G., Salgado, R., Dutra, E., Boussetta, S., Stockdale, T., Potes, M.: On the
870 contribution of lakes in predicting near-surface temperature in a global weather
871 forecasting model. *Tellus A: Dynamic Meteorology and Oceanography*.
872 <https://doi.org/10.3402/tellusa.v64i0.15829>, 2012

873 Balsamo, G., Interactive lakes in the Integrated Forecast System. ECMWF Newsletter
874 137, p. 30-34. 10.21957/rffv1gir, 2013.

875
876 Balsamo, G., Mahfouf, J.-F.: Les schémas de surface continentale pour le suivi et la
877 prévision du système Terre au CEPMMT. *La Météorologie*, 108, 77-81, 2020.

878
879 Belovsky, G., Stephens, D., Perschon, C., et al.: The Great Salt Lake Ecosystem (Utah,
880 USA): long term data and a structural equation approach, *Ecosphere*, 2, 1-40,
881 <doi.org/10.1890/ES10-00091.1>, 2011.

882
883 Benjamin, S.G., D. Devenyi, S.S. Weygandt, K.J. Brundage, J.M. Brown, G. Grell, D.
884 Kim, B.E. Schwartz, T.G. Smirnova, T.L. Smith, G.S. Manikin: An hourly
885 assimilation/forecast cycle: the RUC. *Mon. Wea. Rev.*, 132, 495-518. 2004.

886
887 Benjamin, S.G., B.D. Jamison, W.R. Moninger, S. R. Sahm, B. Schwartz, T.W.
888 Schlatter: Relative short-range forecast impact from aircraft, profiler, radiosonde, VAD,
889 GPS-PW, METAR, and mesonet observations via the RUC hourly assimilation
890 cycle. *Mon. Wea. Rev.*, 138, 1319-1343. 2010.

891
892 Benjamin, S. G., S.S. Weygandt, M. Hu, C.A. Alexander, T.G. Smirnova, J.B. Olson,
893 J.M. Brown, E. James, D.C. Dowell, G.A. Grell, H. Lin, S.E. Peckham, T.L. Smith, W.R.
894 Moninger, G.S. Manikin: A North American hourly assimilation and model forecast
895 cycle: The Rapid Refresh. *Mon. Wea. Rev.*, 144, 1669-
896 1694. <http://dx.doi.org/10.1175/MWR-D-15-0242.1>. 2016.

897
898 Benjamin, S.G., E.P. James, M. Hu, C.R. Alexander, T.T. Ladwig, J.M. Brown, S.S.
899 Weygandt, D.D. Turner, P. Minnis, W.L. Smith, Jr., and A. Heidinger: Stratiform cloud-
900 hydrometeor assimilation for HRRR and RAP model short-range weather prediction.
901 *Mon. Wea. Rev.*, 149, 2673-2694. <https://doi.org/10.1175/MWR-D-20-0319.1>. 2021.

902
903 Benjamin, S.G., T.G. Smirnova, E.P. James, L.-F. Lin, M. Hu, D.D. Turner, and S. He:
904 Land-snow assimilation including a moderately coupled initialization method applied to
905 NWP. *J. Hydromet.*, 23, 825-845. <https://doi.org/10.1175/JHM-D-21-0198.1>, 2022.

906
907 Boussetta, S.; Balsamo, G.; Arduini, G.; Dutra, E.; McNorton, J.; Choulga, M.; Agustí-
908 Panareda, A.; Beljaars, A.; Wedi, N.; Muñoz-Sabater, J.; de Rosnay, P.; Sandu, I.;
Hadade, I.; Carver, G.; Mazzetti, C.; Prudhomme, C.; Yamazaki, D.; Zsoter, E.:
ECLand: The ECMWF Land Surface Modelling System. *Atmosphere*, 12, 723.
<https://doi.org/10.3390/atmos12060723>, 2021.

Formatted: Header

Formatted: English (US)

Formatted: Font: Not Bold

Formatted: Font: Not Bold

Formatted: Font: Not Bold

Formatted: Font: Not Bold

Formatted: Border: Top: (No border), Bottom: (No border), Left: (No border), Right: (No border), Between : (No border)

Deleted: *Hydromet.*, 23, accepted.

Formatted: Font color: Auto

Formatted: Font color: Auto

- Charusombat, U., Fujisaki-Manome, A., Gronewold, A. D., Lofgren, B. M., Anderson, E. J., Blanken, P. D., Spence, C., Lenters, J. D., Xiao, C., Fitzpatrick, L. E., and Cutrell, G.: Evaluating and improving modeled turbulent heat fluxes across the North American Great Lakes, *Hydrol. Earth Syst. Sci.*, 22, 5559–5578, <https://doi.org/10.5194/hess-22-5559-2018>, 2018.
- Chen, C., Beardsley, R. C., & Cowles, G.: An unstructured grid, finite volume coastal ocean model (FVCOM) system. *Oceanography*, 19(1), 78–89. <https://doi.org/10.5670/oceanog.2006.92>, 2006.
- Chen, C., Beardsley, R., Cowles, G., Qi, J., Lai, Z., Gao, G., et al.: An unstructured grid, Finite-Volume Coastal Ocean Model FVCOM -- User Manual. *Tech. Rep., SMAST/UMASSD-13-0701, Sch. for Mar. Sci. and Technol., Univ. of Mass. Dartmouth, New Bedford.*, 416 pp., 2013
- Choulga, M., Kourzeneva, E., Balsamo, G., Boussetta, S., and Wedi, N.: Upgraded global mapping information for earth system modelling: an application to surface water depth at the ECMWF, *Hydrol. Earth Syst. Sci.*, 23, 4051–4076, <https://doi.org/10.5194/hess-23-4051-2019>, 2019.
- De Pondeca, M.S.F.V., Manikin, G.S., DiMego, G., Benjamin, S.G., Parrish, D.F., Purser, R.J., Wu, W.-S., Horel, J.D., Myrick, D.T., Lin, Y., Aune, R.M., Keyser, D., Colman, B., Mann, G., and Vavra, J.: The Real-Time Mesoscale Analysis at NOAA's National Centers for Environmental Prediction: Current status and development. *Wea. Forecasting*, 26, 593-612, <https://doi.org/10.1175/WAF-D-10-05037.1>, 2011
- Dirmeyer, P.A., Halder, S., Bombardi, R.: On the harvest of predictability from land states in a global forecast model. *J. Geophys. Res. Atmospheres*, 123, 13,111-13,127. <https://doi.org/10.1029/2018JD029103>, 2018.
- Dowell, D. C., C. R. Alexander, E. P. James, S. S. Weygandt, S. G. Benjamin, G. S. Manikin, B. T. Blake, J. M. Brown, J. B. Olson, M. Hu, T. G. Smirnova, T. Ladwig, J. S. Kenyon, R. Ahmadov, D. D. Turner, and T. I. Alcott: The High-Resolution Rapid Refresh (HRRR): An hourly updating convection-allowing forecast model. Part I: Motivation and system description. *Wea. Forecasting*, 150, <https://doi.org/10.1175/WAF-D-21-0151.1>, 2022.
- Downing, J.A. et al: The global abundance and size distribution of lakes, ponds, and impoundments. *Limnol. Oceanogr.*, 51, 2388-2397. 2006.
- Dutra, E., Stepanenko, V. M., Balsamo, G., Viterbo, P., Miranda, P. M and co-authors: An offline study of the impact of lakes on the performance of the ECMWF surface scheme. *Boreal Env. Res.* 15, 100–112, 2010.

Deleted: Forecasting, accepted with revision.

Formatted: Font: Not Italic, Font color: Auto, Pattern: Clear

- ECMWF, OpenIFS: Lakes,
<https://confluence.ecmwf.int/display/OIFS/3.5+OpenIFS:+Lakes>. Accessed 7 Dec 2021,
 2020.
- Fiedler, E.K., Martin, M.J., Roberts-Jones, J.: An operational analysis of Lake Surface
 Water Temperature. *Tellus A*, 6, <https://doi.org/10.3402/tellusa.v66.21247>, 2014.
- Fujisaki-Manome, A., G. E. Mann, E. J. Anderson, P. Y. Chu, L. E. Fitzpatrick, S. G.
 Benjamin, E. P. James, T. G. Smirnova, C. R. Alexander, and D. M. Wright:
 Improvements to lake-effect snow forecasts using a one-way air-lake model coupling
 approach. *J. Hydrometeor.*, **21**, 2813-2828, <https://doi.org/10.1175/JHM-D-20-0079.1>,
 2020.
- Gao, G., C. Chen, J. Qi, and R. C. Beardsley: An unstructured-grid, finite-volume sea
 ice model: Development, validation, and application. *J. Geophys.*
Res., **116**, C00D04, <https://doi.org/10.1029/2010JC006688>. 2011.
- Gemmill, W., B. Katz, and X. Li: Daily real-time, global sea surface temperature—High-
 resolution analysis: RTG_SST_HR. NCEP Office Tech. Note 260, 39 pp. Available
 online at <http://polar.ncep.noaa.gov/mmab/papers/tn260/MMAB260.pdf> , 2007.
- Gu, H., Jin, J., Wu, Y., Ek, M.B., and Subin, Z.M.: Calibration and validation of lake
 surface temperature simulations with the coupled WRF-lake model. *Climatic Change*,
 129, 471-483. DOI 10.1007/s10584-013-0978-y, 2015.
- Hamill, T.M.: Benchmarking the raw model-generated background forecast in rapidly
 updated surface temperature analyses. Part I: Stations. *Mon. Wea. Rev.*, **148**, 689-
 700. <https://doi.org/10.1175/MWR-D-19-0027.1>, 2020.
- Hostetler, S.W., Bates, G., Giorgi, F.: Interactive coupling of a lake thermal model with
 a regional climate model. *J. Geophys. Res.*, 98, 5045-5057. DOI:[10.1029/92JD02843](https://doi.org/10.1029/92JD02843),
 1993.
- Hunter, T. S., Clites, A. H., Campbell, K. B., & Gronewold, A. D.: Development and
 application of a monthly hydrometeorological database for the North American Great
 Lakes - Part I: precipitation, evaporation, runoff, and air temperature. *Journal of Great
 Lakes Research*, 41(1), 65–77, 2015
- James, E. P., and S. G. Benjamin: Observation system experiments with the hourly
 updating Rapid Refresh model using GSI hybrid ensemble-variational data
 assimilation. *Mon. Wea. Rev.*, **145**(8), 2897-2918. <https://doi.org/10.1175/MWR-D-16-0398.1>, 2017.
- James, E. P., C. R. Alexander, D. C. Dowell, S. S. Weygandt, S. G. Benjamin, G. S.
 Manikin, J. M. Brown, J. B. Olson, M. Hu, T. G. Smirnova, T. Ladwig, J. S. Kenyon, and

1009 D. D. Turner: The High-Resolution Rapid Refresh (HRRR): An hourly updating
1010 convection-allowing forecast model. Part II: Forecast performance. *Wea. Forecasting*,
1011 **150**, <https://doi.org/10.1175/WAF-D-21-0130.1>, 2022.

1012
1013 Kelley, S.G.T, J.G.W. Kelley, and E.J. Anderson: Evaluation of the NASA SPoRT
1014 Composite Product of surface water temperatures for large lakes in New England and
1015 New York State. *Abstract, 24th Conference on Satellite Meteorology, Oceanography,*
1016 *and Climatology*. Available at
1017 <https://ams.confex.com/ams/101ANNUAL/meetingapp.cgi/Paper/381301>, 2021.

1018
1019 Kourzeneva, E., Martin, E., Batrak, Y., LeMoigne, P. Faroux: Climate data for
1020 parameterisation of lakes in Numerical Weather Prediction models, *Tellus A.*, 64: . DOI:
1021 [10.3402/tellusa.v64i0.17226](https://doi.org/10.3402/tellusa.v64i0.17226), 2012a.

1022
1023 Kourzeneva, E., Asensio, H., Martin, E., Faroux: Global gridded dataset of lake
1024 coverage and lake depth for use in numerical weather prediction and climate modelling.
1025 *Tellus A.*, 64: 15640. [10.3402/tellusa.v64i0.15640](https://doi.org/10.3402/tellusa.v64i0.15640), 2012b.

1026
1027 Lawrence, D. M., Fisher, R. A., Koven, C. D., Oleson, K. W., Swenson, S. C., Bonan,
1028 G., et al.: The Community Land Model version 5: Description of new features,
1029 benchmarking, and impact of forcing uncertainty. *Journal of Advances in Modeling Earth*
1030 *Systems*, 11, 4245–4287. <https://doi.org/10.1029/2018MS001583>, 2019.

1031
1032 Lewis, W. M., Jr.: A revised classification of lakes based on mixing. *Can. J. Fish.*
1033 *Aquat. Sci.* 40, 1779–1787. <https://doi.org/10.1139/f83-207>, 1983

1034
1035 Mallard, M.S., Nolte, C.G., Spero, T.L., Bullock, O.R., Alapaty, K., Herwehe, J.A., Gula,
1036 J., Bowden, J.H.: Technical challenges and solutions in representing lakes when using
1037 WRF in downscaling applications. *Geosci. Model Dev.*, 8, 1085–1096, 2015.

1038
1039 Mironov, D., Heise, E., Kourzeneva, E., Ritter, B., Schneider, N., and Terzhevik, A.:
1040 Implementation of the lake parameterisation scheme FLake into numerical weather
1041 prediction model COSMO, *Boreal Environ. Res.*, 15, 218–230, 2010.

1042
1043 Muñoz-Sabater, J., H. Lawrence, C. Albergel, P. de Rosnay, L. Isaksen, S.
1044 Mecklenburg, Y. Kerr, and M. Drusch: Assimilation of SMOS brightness temperatures in
1045 the ECMWF Integrated Forecasting System. *Quart. J. Roy. Meteor. Soc.*, **145**, 2524–
1046 2548, <https://doi.org/10.1002/QJ.3577>, 2019.

1047
1048 NASA: Surface water temperature composite.
1049 <https://weather.msfc.nasa.gov/sport/sst/>. Downloaded 2 Nov 2021, 2021

1050
1051 National Weather Service: Service Change Notice 20-10. Available at
https://www.weather.gov/media/notification/scn20-10nsst1_0.pdf, 2020.

Formatted: Header

Deleted: Forecasting., accepted with revision,

Formatted: Font color: Auto, Pattern: Clear

Deleted: 2012

Formatted: Font: Italic

Deleted: FLake

1055 Pondeva, M.S.F.V. de, G.S. Manikin, G. DiMego, S.G. Benjamin, D.F. Parrish, R.J.
 1056 Purser, W.-S. Wu, J. Horel, Y. Lin, R.M. Aune, D. Keyser, L. Anderson, B. Colman, G.
 1057 Mann, and J. Vavra: The Real-Time Mesoscale Analysis at NOAA's National Centers
 1058 for Environmental Prediction: Current Status and Development. *Wea. Forecasting*, **26**,
 1059 593-612. 2011.

1060 Powers, J. G., and Coauthors: The Weather Research and Forecasting Model:
 1061 Overview, system efforts, and future directions. *Bull. Amer. Meteor. Soc.*, **98**, 1717-
 1062 1737, <https://doi.org/10.1175/BAMS-D-15-00308.1>, 2017

1063 Railsback, B.: Some fundamentals of mineralogy and geochemistry. Figure on lake
 1064 salinity at <http://railsback.org/Fundamentals/SFMGLakeSize&Salinity071.pdf>, 2006

1065 Skamarock, W. C., and Coauthors, 2019: A description of the Advanced Research WRF
 1066 version 4. NCAR Tech. Note NCAR/TN-556+STR, 162 pp., [Available online at
 1067 http://www2.mmm.ucar.edu/wrf/users/docs/technote/v4_technote.pdf]. 2019.

1068 Subin, Z. M., Riley, W. J., & Mironov, D.: An improved lake model for climate
 1069 simulations: Model structure, evaluation, and sensitivity analyses in CESM1. *Journal of*
 1070 *Advances in Modeling Earth Systems*, 4(1). <https://doi.org/10.1029/2011ms000072>,
 1071 2012.

1072 Thiery, W., Stepanenko, V., Fang, X., Jöhnk, D., Li, Z., Martynov, A., Perroud, M.,
 1073 Subin, Z., Darchambeau, F., Mironov, D., Van Lipzig, N.: LakeMIP Kivu: evaluating the
 1074 representation of a large, deep tropical lake by a set of one-dimensional lake models,
 1075 *Tellus A: Dynamic Meteorology and Oceanography*, 66:1, 21390, DOI:
 1076 10.3402/tellusa.v66.21390, 2014.

1077 U.S. National Ice Center, updated daily: *IMS Daily Northern Hemisphere Snow and Ice*
 1078 *Analysis at 1 km, 4 km, and 24 km Resolutions, Version 1*. Boulder, Colorado USA.
 1079 NSIDC: National Snow and Ice Data Center.
 1080 [Doi: https://doi.org/10.7265/N52R3PMC](https://doi.org/10.7265/N52R3PMC). Accessed 8 November 2021, 2021.

1081 Vanderkelen, I., van Lipzig, N. P. M., Sacks, W. J., Lawrence, D. M., Clark, M.,
 1082 Mizukami, N., Pokhrel, Y., and Thiery, W.: The impact of global reservoir expansion on
 1083 the present-day climate, EGU General Assembly 2021, online, 19–30 Apr 2021,
 1084 EGU21-723, <https://doi.org/10.5194/egusphere-egu21-723>, 2021

1085 Verpoorter, C., Kutser, T., Seekell, D.A., and Tranvik, L.J.: A global inventory of lakes
 1086 based on high-resolution satellite imagery. *Geophys. Res. Lett.*, 41, 6396–6402,
 1087 doi:10.1002/2014GL060641. 2014.

Formatted: Header

Deleted: NOAA's

Formatted: Font color: Auto

Formatted: Normal

Deleted: doi

1098 Wang, F., Ni, G., Riley, W. J., Tang, J., Zhu, D., and Sun, T.: Evaluation of the WRF
 1099 lake module (v1.0) and its improvements at a deep reservoir, *Geosci. Model Dev.*, 12,
 1100 2119–2138, <https://doi.org/10.5194/gmd-12-2119-2019>, 2019.
 1101
 1102 Weygandt, S. S., S. G. Benjamin, M. Hu, C. R. Alexander, T. G. Smirnova, and E. P.
 1103 James: Radar reflectivity-based model initialization using specified latent heating
 1104 (Radar-LHI) within a diabatic digital filter or pre-forecast integration. *Wea. Forecasting*,
 1105 **150**, <https://doi.org/10.1175/WAF-D-21-0130.1>, 2022.
 1106
 1107 Wilson, R. C., Hook, S. J., Schneider, P., and Schladow, S. G.: Skin and bulk
 1108 temperature difference at Lake Tahoe: A case study on lake skin effect. *J. Geophys.*
 1109 *Res. Atmos.*, 118, 10,332–10,346, <https://doi.org/10.1002/jgrd.50786>, 2013.

Formatted: Header

Deleted: Forecasting, accepted with revision,

Formatted: Font: Not Italic, Font color: Auto, Pattern:
Clear

Page 4: [1] Deleted Stan Benjamin 6/21/22 6:49:00 AM

Page 4: [1] Deleted Stan Benjamin 6/21/22 6:49:00 AM

Page 4: [1] Deleted Stan Benjamin 6/21/22 6:49:00 AM

Page 4: [2] Deleted Stan Benjamin 6/21/22 6:49:00 AM

Page 4: [2] Deleted Stan Benjamin 6/21/22 6:49:00 AM

Page 4: [2] Deleted Stan Benjamin 6/21/22 6:49:00 AM